2014 IEEE 28-th Convention of Electrical and Electronics Engineers in Israel

PERFORMANCE MEASURES FOR SPARSE SPIKE INVERSION VS. BASIS PURSUIT INVERSION

Igal Rozenberg
Technion – IIT
Haifa, Israel
igalroz@tx.technion.ac.il

Israel Cohen
Technion – IIT
Haifa, Israel
icohen@tx.technion.ac.il

Anthony Vassiliou
GeoEnergy, Inc.
Houston TX, USA
anthony@geoenergycorp.com

Abstract—**Sparse Spike Inversion (SSI) and Basis Pursuit Inversion (BPI) are two methods for seismic inversion which utilize sparse inversion techniques. A LARS-LASSO solver is used for comparison of their performances. We propose the use of the F-measure to better evaluate the methods' capability to correctly identify reflections from layers' boundaries. We also show that flexible l1 penalization in the LASSO solution holds potential for improving performance.**

Keywords—seismic inversion, sparse spike inversion, basis pursuit inversion

1 INTRODUCTION

In the seismic inversion problem we aim to find the ground layers' structure from measurements of acoustic echoes of a given, or estimated, signal.

A short seismic pulse is transmitted from the earth surface. A sensor array deployed on the ground receives the reflected pulses from the interface between ground layers with different impedance. Following some simplifying assumption and a pre-processing stage, the data can be regarded as a series of one dimensional traces. In this 1D forward model ([8],[7]), a seismic wavelet is convolved with the reflectivity series to produce the seismic trace. The reflectivity pattern is assumed to be sparse as only boundaries between adjacent layers may cause a reflection of the seismic wave. It is desirable to perform a de-convolution of the seismic traces to obtain estimates of the reflectivity patterns. As noted in the literature, the band limited seismic wavelet imposes limitation on the accuracy of the inversion processes; specifically, high frequencies components of the reflected wave may be more susceptible to noise or may not be retrievable at all. It was suggested to use inversion techniques which inherently exploit the sparsity of the reflection channels.

In this paper, we examine the Sparse Spike Inversion (SSI) and the Basis Pursuit Inversion (BPI) [1]. Both methods use a dictionary of expected signal forms, based on the estimated seismic wavelet. The solution for both methods is based on the LASSO convex relaxation of the classical sparse inversion problem. We compare the performances of these two methods under various scenarios. We suggest the F-measure, a fidelity criterion additional to the correlation, to evaluate the algorithms performances. We also refer to the sparsity promoting l1-penalty term of the LASSO. We show that a variable selection of the penalty for each specific trace can improve the result compared to a fixed penalty even for fixed SNR scenario. In addition, we observe that the selection of the dictionary resolution for the inversion process, can greatly affects the algorithms' performances. Lastly, based on our observed results we suggest further research directions.

The paper is organized as follows. In Section 2, we introduce the mathematical model and the mathematical approach for the solution. In Section 3, we refer to several implementation issues in the sparse solution approach. In Section 4, we introduce the simulation results and fidelity criteria. In Section 5, we demonstrate experimental results.

2 MODELING AND SOLUTION APPROACHES

We adopt the 1-D "forward model" also utilized in [1]

$$(2.1)\quad s(t) = w(t) * r(t) + n(t)\,.$$

According to this model, the earth structure is laminated in planar horizontal layers. Each such layer is assumed to have uniform characteristics or "impedance". An acoustic signal $w(t)$ traveling within this medium will exhibit reflections at the boundaries of such layers with different impedances. Thus, the reflectivity pattern $r(t)$ encapsulates the desired data on the ground's structure.

In typical scenarios, $r(t)$ is a sparse signal. The seismic wavelet $w(t)$ is assumed to be known. Practically it is estimated in a pre-processing stage. The measured signal is the convolution of the seismic wavelet with the reflectivity pattern. Random additive noise with supposedly known statistics often contaminates the measurement. The final measurement $s(t)$ is usually referred to as the seismic trace. The objective of the inversion is to find the reflectivity $r(t)$ from the seismic trace $s(t)$. The seismic wavelet $w(t)$ is band limited in its nature. Hence, even in the absence of noise one can hope to recover $r(t)$ up to the bandwidth resolution $w(t)$ permits. In practice this translates to a minimal layer thickness below which we do not expect to detect.

In this paper, we examine the performance of two techniques aimed to recover the reflectivity pattern, namely SSI and BPI [1]. In the following, we briefly present the models and the solution approach. We refer the reader to [1] for further details. Both the SSI and BPI rely on the knowledge of the seismic wavelet $w(t)$. As (2.1) implies, the seismic trace consists of a sum of $w(t)$ and its time shifts, according to the non-zero reflectors in $r(t)$. After time discretization, and an addition of random noise, (2.1) takes the form of:

$$(2.2)\ s_{N\times 1} = W_{N\times M} r_{M\times 1} + n_{N\times 1}.$$

In the SSI inversion method, $W_{N\times M} \in \mathbb{R}^{N\times M}$, also known as the Dictionary, is the convolution matrix formed column by column by samples' shifts of the seismic wavelet $w[k]$. The j-th column of $W_{N\times M}$ can be seen as the measured response to a clean "reflection impulse" at time j: $r^{\delta-j}[k] = \delta[k-j]$. N is the number of measurements in the seismic trace. M is the discretized possible locations of layers' boundaries.

The BPI method is aimed to capture thinner layers. As such, Zhang and Castagna [1] propose to construct the Dictionary $W_{N\times M}$ as even and odd wedge reflectivity pairs. Essentially the BPI Dictionary is comprised of a discretized ($t = k\Delta T_s$) version of the signals:

$$(2.3)\ A_e(t,m,n,\Delta T_s) = w(t) * \left[\delta(t - m\Delta T_s) + \delta(t - m\Delta T_s - n\Delta T_s)\right]$$

for the even atoms, and similarly

$$(2.4)\ A_o(t,m,n,\Delta T_s) = w(t) * \left[\delta(t - m\Delta T_s) - \delta(t - m\Delta T_s - n\Delta T_s)\right]$$

for the odd atoms. The indexes m,n assume all the legitimate values. The inversion problem of finding $r_{M\times 1}$ from the noisy measurement $s_{N\times 1}$ is formulated as

$$(2.5)\ \min \left\|r_{M\times 1}\right\|_0 \ subject\ to \left\|s_{N\times 1} - W_{N\times M} r_{M\times 1}\right\|_2^2 < \varepsilon.$$

The convex relaxation of (2.5) after an additional Lagrangian relaxation of the constraint is given by:

$$(2.6)\ \min_{r_{M\times 1}} \frac{1}{2}\left\|s_{N\times 1} - W_{N\times M} r_{M\times 1}\right\|_2^2 + \lambda \left\|r_{M\times 1}\right\|_1.$$

The problem formulated in the form of (2.6) is named "LASSO". The use of l1 penalty in similar support recovery problems proved to promote sparsity (see [2], [3]) of the solution $r_{M\times 1}$.

3 SIMULATION SETTINGS

Both the SSI and BPI methods were simulated. We focused on performance evaluation of the SSI and BPI methods for inversion on synthetic data under various settings. In this section, we describe the following aspects of the simulation environment: (i) Synthetic generation of the reflection channel and the seismic wavelet; (ii) Generation of the seismic trace; (iii) The dictionary; (iv) LARS-LASSO solver. We note that we were aided by [1] for choosing some of the simulation parameters

I. Synthetic generation of the reflection channel the seismic wavelet

The simulation was performed in two operational sampling rates of 500Hz and 166.667Hz. Most results shown were taken from the 500Hz setting. The Ricker wavelet of 40Hz bandwidth served as the seismic wavelet. Its sampled version[1] with $L_W = round(25 \cdot (F_s / 500))$ samples is denoted by $w[k]$. The reflectivity pattern maximal delay was set to 0.5sec. Hence, For the aforementioned sampling rates F_s, the reflection pattern $r[k]$ translates into a 251 taps and 84 taps FIR filters, respectively. The channel coefficients were generated in pairs with a fixed but customizable delay D_p. This spacing between adjacent reflections is a crucial factor in the inversion algorithms. Hence we would rather control this spacing rather than setting it at random to better evaluate the methods' performances. Another customizable parameter is the channels' sparsity (p). The delay between one pair to the next adjacent one was randomly chosen as $D_p + \Delta(p)$ where $\Delta(p) \sim Geom(p)$. When we question the effects of the different sampling rate, the reflection channels were synthesized in the low sampling rate and up-converted to the higher rate by adding zeros between samples. This scheme allows a fair comparison of the two as the number of reflections is kept constant. Lastly, the magnitude of each reflection was drawn independently from a uniform distribution in the range [-0.2, 0.2].

II. Generation of the seismic trace

Once the seismic wavelet and the reflectivity pattern are set, the generation of the seismic trace is rather straightforward. Yet we want to focus attention on some fine details. The seismic trace is generated by convolving the seismic wavelet $w[k]$ with the reflectivity pattern $r[k]$. Then, an additive $n[k]$ IID zero-mean Gaussian noise with pre-specified variance matrix, say $\sigma_n^2 I_{L_T\times L_T}$,is added to obtain the seismic trace $s[k]$. The variance is chosen to reach a desired SNR:

$$(2.7)\ s[k] = w[k] * r[k] + n[k].$$

Since we are dealing with sparse inversion techniques, it is not only the SNR that matters but also the distribution and magnitude of the reflectivity coefficients $r[k]$. We take a standard approach and set the noiseless response to have a unit norm $\left\|w[k] * r[k]\right\|_2^2 \to 1$. Then, the noise is generated such that $E\left\|n[k]\right\|_2^2 = \frac{1}{SNR}$

III. The Dictionary

The Dictionary is synthesized according to the guidelines explained in the previous section. We keep in mind that $r[k]$ is an L_{FIR} length vector, the seismic wavelet $w[k]$ is an L_W length vector. We denote by $r^{\delta-j}[k] = \delta[k-j]$ the L_{FIR} length vector with a single non-zero unit value at $k = j$. Then, The SSI dictionary $W_{Ns\times Ms}^{SSI}$ j-th column is simply given by: $w[k] * r^{\delta-j}[k]$. The BPI dictionary $W_{Nb\times Mb}^{BPI}$ synthesis is a bit more involved as it should include all the possible odd and even pairs responses to the seismic wavelet as implied by (2.3) and (2.4). Let L_{FIR} be the channel length, then the total number of dictionary atoms Nb is given

[1] $w[k]$ was generated with the aid of the MATLAB© function s=ricker(npt,freq,dt,nsw).No tapering was used and so nsw was set to 0.

by $Nb = 2\sum_{l=1}^{L-1}(L_{FIR} - l - 1) + L_{FIR}$. The first term corresponds to all even (and odd) pairs deployment over the channel; For a pair with its early reflection at time index l, we identify $2(L_{FIR} - l + 1)$ possible late reflection companions. The second term corresponds to the single reflection scenario where the late pair companion is outside the FIR scope. This second part is, as a matter of fact, a duplication of the SSI dictionary. Practically, for the sake of reducing computation time, we synthesized the dictionary by taking only reflection pairs with spacing lower or equal to 12 taps.

We note that the shift-invariance property of atoms' groups in the dictionary could be utilized to reduce complexity of the inversion algorithms

IV. LARS-LASSO solver

The LARS algorithm [4] can be adjusted to solve the LASSO (2.6) for the whole path of λ. The LARS method alternately augments or, at times, drops, atoms from the active support of $r_{M\times 1}$. Uniqueness of the solution is guaranteed by convexity [5, 3]. In our simulation, we used the SpaSM toolbox [6] for both the SSI and BPI inversion methods.

We call the function 'lasso.m'[2] with $'X'$ being either the SSI or BPI dictionary, $'y'$ the seismic trace and $'stop = 0'$ so that we get the whole λ path. The function has two outputs - $'b'$ and 'info' The output $'b'$ is a matrix of size $L_{FIR} \times P$ where L_{FIR} is the number of reflection coefficients (251). P is the number of junction points[3]. The 1st column of 'b' is always the zero vector corresponding to the $\lambda \to \infty$ solution. The 'lasso.m' function calls an internal function 'larsen.m'

We made the following modifications in 'larsen.m':

1. (Larsen.m-l.36) `maxSteps = 12*maxVariables;`
2. (Larsen.m-l.13) Adding to the while loop a lower limit criteria to the residual's norm $\|r\|_2 > 1e-6$.
3. (Larsen.m-l.63) The error message in case of 'no positive direction' is replaced by a warning and a 'break' command.
4. (Larsen.m) The unbiased LS solution based on the support of 'b' is calculated and given as output of 'lars.m' (see [3], p. 100).

The first three modifications were needed to enable calculation of a significant part of the λ route while maintaining numerical stability. These changes became inevitable in the highly correlated BPI dictionary. The use of the unbiased LS solution gave a small improvement of the simulation results. The above modifications both contribute to the stability of the simulation and reduce the execution runtime.

[2] [b info]=lasso(X, y, stop, storepath, verbose)

[3] "Junction" – λ where new atom is augmented or an active atom is dropped.

4 FIDELITY CRITERIA AND EXPERIMENTAL RESULTS

Based on the aforementioned settings, we evaluated the performances of the SSI and BPI methods on synthesized random channels with random noise .

We simulated several scenarios with different SNRs, channels' sparsity p, and spacing between reflected pairs D_p. We also show the possible importance of varying simulation sampling rate on the inversion performance. Simulation results for various triplets (SNR,p, D_p) are given below under different settings. For each scenario, we ran 100 tests. Two fidelity criteria, sometimes referred to as performance measures, were used to evaluate the performance in the different scenarios. The first criterion, also adopted by [1], is the average correlation between the actual reflectivity $r[n]$ and its estimate $\hat{r}[n]$:

$$(2.8)\ \rho_{corr} = \frac{< r[n], \hat{r}[n] >}{\|r[n]\|_2 \cdot \|\hat{r}[n]\|_2}.$$

The second fidelity criterion offers a qualitative measure of the accuracy of the estimated layers' structure. Ultimately, one wishes to identify the locations of the interfaces between adjacent layers; In the mathematical model (2.2), this translates into a correct identification of the support of $r[n]$. Using the standard definitions of precision and recall, we use a modified version of the "F measure" to estimate the performance of the support recovery:

$$F = \frac{\mathrm{Pr}ecision \cdot \mathrm{Re}call}{\frac{1}{2}\left(\mathrm{Pr}ecision + \mathrm{Re}call\right)} = \frac{TP}{TP + \frac{1}{2}(FP + FN)}.$$

The F measure takes a value in the range $0 \le F \le 1$. As the F-measure relies on dichotomic values of the reflection coefficients – zero or nonzero, some thresholding is necessary to mitigate the effects of noise and even numerical sensitivities. This basic, yet effective post-processing, greatly improves the active support detection. The minimum value γ we selected for a reflection coefficient to be considered active was set to:

$$(2.9)\ \gamma = \min\left\{\sqrt{\frac{1}{10}\frac{\sigma_s^2}{L_{FIR} \cdot p} + 0.5 \cdot \sigma_n^2},\ 10 \cdot \sigma_n\right\}.$$

For sparsity p and signal variance σ_s^2, the average reflection coefficient amplitude for non time overlapping reflections would be $O\left(\sqrt{\frac{\sigma_s^2}{pL_{FIR}}}\right)$. In practice, the high correlation between adjacent atoms, mostly observed in small D_p scenarios, may end up in smaller amplitudes. The expected contribution of the noise to a specific reflection coefficient is $O(\sigma_n^2)$. Thus, a reasonable threshold for reflection coeffi-

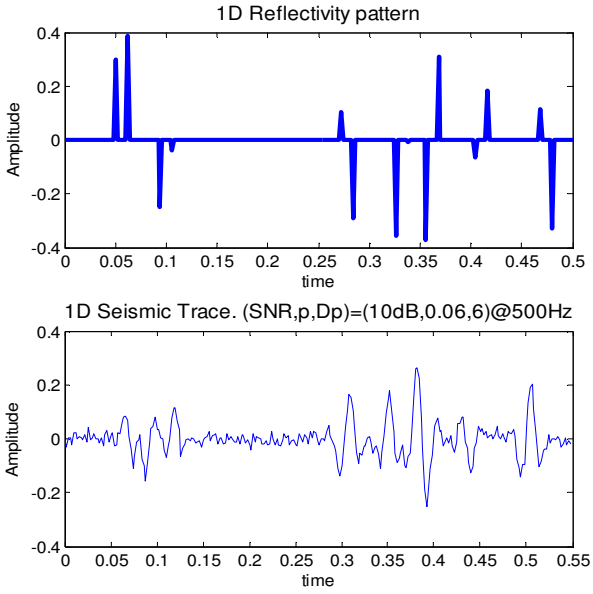

Figure 1 - Synthetic reflection channel and its corresponding noisy seismic trace.

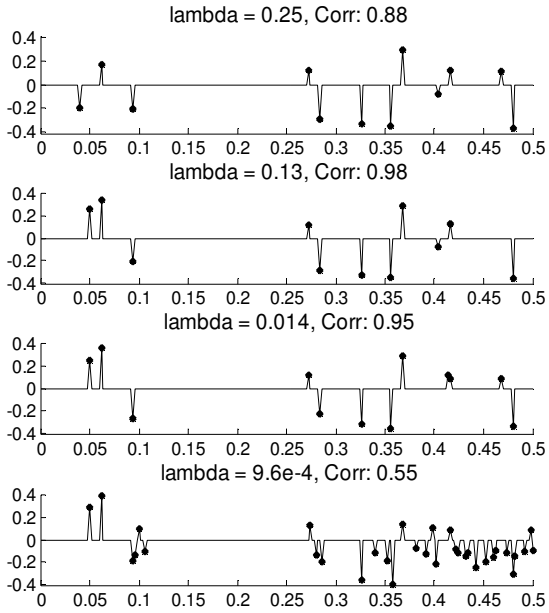

Figure 2 - Reconstructed reflection channel Coefficients for different λ values (thresholded coefficients).

cient amplitude may take the form: $\sqrt{A\frac{\sigma_s^2}{L_{FIR}\cdot p}+B\cdot\sigma_n^2}$

where different

selections of A, B reflect a tradeoff between possible misdetection and possible false detection.

The first term in γ, inherently introduces misdetection even in the noiseless case; hence, for scenarios with very high SNRs, a limit of $10\sigma_n$ was set to significantly reduce such misdetections.

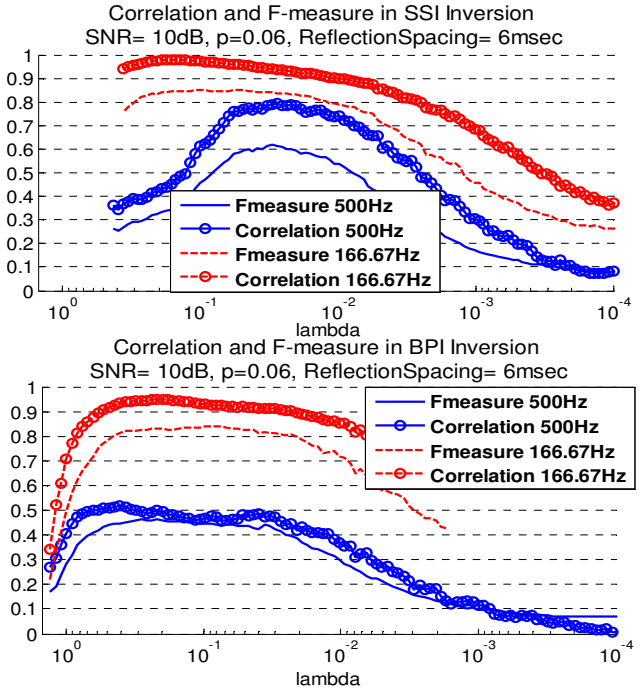

Figure 3 – Comparison of SSI and BPI methods - Average performance for fixed λ values and 100 runs.

In the first simulation setting we evaluate the correlation factor and F-measure by averaging results for a specific (logarithmic) set of λ[4]. Table 1 shows simulation results in this setting. For each triplet we get an average performance for each corresponding λ. The values in the table are the λ values which correspond to the maximal performance measures extracted for each scenario. The correlation measure is also compared to an oracle scenario where the actual support is given and LS estimation is applied. In Figure 3, the performances of the two fidelity measures are presented for a whole set of λ for a given scenario [triplet (SNR,p, D_p)].

During the above simulations it became apparent that the maximal correlation or most accurate support recovery is achievable at different values of λ for different channels' inversion. This can be accounted for the different number of reflections, the spacing between them, the varying reflection coefficients' magnitude and noise. Following this observation, each of the two fidelity criteria was evaluated under an additional setting.

In the second simulation setting, whose results are partially given in Table 2, we register for each specific channel inversion the actual value of λ for which the performance measures actually achieve their maximal values. Interpolation of the measured performance to a fixed grid of λ-s then follows. When repeated for various channels, we get joint distributions: for $(\lambda_{\rho-\max}, \rho_{\max})$ and for $(\lambda_{F-\max}, F_{\max})$. This second setting is applied only for the low $SNR = 10dB$ scenarios, since for high SNR scenarios we already observe almost per-

[4] Average performance measures are evaluated for λ on a fixed grid points for which we have a minimum statistics from $N_{trials}/2 = 50$ different runs

fect recovery for some fixed λ . We also keep in mind that in practice the best matching λ is not accessible but instead a smart stopping criterion for the LARS-LASSO should be applied to maximize performance. In the scope of this paper we do not present the whole results of the second setting simulation. Yet we report a consistent improvement in the inversion performance where the variance between different runs is much smaller than the improvement rate.

In trying to understand the partial gap in performance between the reported results in [1] and our simulation results another test was performed. This test involves a change in the simulation sampling rate and hence dictionary atoms and the spacing between them. Figure 3 demonstrates that the inversion performance is quite substantially influenced by the operational sampling rate. For the same SNR and reflectance patterns statistics, it is observed that a lower sampling rate in the order of twice of the seismic wavelet Nyquist rate, performs better than the densely sampled one. We see that both SSI and BPI "suffer" from over-sampled dictionaries but BPI is more sensitive. We believe that the sampling rate and dictionary atoms depend not only on the seismic wavelet bandwidth but also on the measurement SNR and the inversion resolution we aim to achieve.

5 DISCUSSION AND FURTHER RESEARCH

The results above reveal several interesting aspects of the sparse channel inversion methods. Also, they give rise to further research directions.

From Table 1 we see that for high enough SNR, the reconstruction in both methods is perfect or very close to that. This result even holds true for pair spacing of 3 taps (at 500Hz) $\Delta t = 3 \cdot \frac{1}{500} = 6m\sec$ which is below the expected separation capabilities of our 40Hz seismic wavelet $\Delta t = \frac{\sqrt{6}}{2\pi f_0} = \frac{\sqrt{6}}{2\pi \cdot 40} = 9.7m\sec$ [1]. Also, following the observation in the previous section, the selection of the dictionary should be considered so as to maximize performance for a given SNR and seismic wavelet.

Another interesting observation which is also apparent is the rather strong correspondence between the λ-s for which the correlation and the F-measure take their maximal values in the noisy low SNR scenarios. In the high SNR case, the peak is quite flat so the actual maximum may not be of great significance. It can be also observed that both fidelity criteria show better recovery for more sparse reflection patterns, higher pair spacing and higher SNRs. Our results also indicate better performance of the SSI technique although with proper dictionary atom selection these differences seem to become significantly smaller. The results above encourage a further investigation of sparse inversion techniques and also a stopping

criterion for the LARS-LASSO algorithm which may be data and SNR dependent. This has a potential for improving the inversion performance compared to the fixed λ case. It is also desirable to further examine the performance of the BPI

Table 1 - Fixed Lambda average Performance (Fs=500Hz).

(SNR,p, D_p) Fs=500Hz	**Max. Correlation ρ** $\lambda_{\max-\rho}$, $\max_{\lambda} E[\rho_\lambda]$			**Max. F-measure** $\lambda_{\max-F}$, $\max_{\lambda} E[F_\lambda]$	
	SSI	BPI	Oracle $\rho_{\max}$	SSI	BPI
(10dB,0.04,3)	(0.02,0.76)	(0.39,0.45)	0.996	(0.022,0.59)	(0.049,0.38)
(10dB,0.04,6)	(0.07,0.95)	(0.12,0.72)	0.996	(0.045,0.80)	(0.19,0.58)
(10dB,0.06,6)	(0.045,0.93)	(0.12,0.71)	0.995	(0.049,0.77)	(0.1,0.57)
(80dB,0.04,3)	(4.7e-6,1)	(5.6e-8,0.99)	1	(2.5e-6,1)	(0.16,0.46)
(80dB,0.04,6)	(3.2e-5,1)	(3.7e-8,0.99)	1	(6.8e-7,1)	(0.31,0.54)

Table 2 - Adaptive Lambda Average Performance (Fs=500Hz).

(SNR,p, D_p) Fs=500Hz	**Max. Correlation ρ** $\lambda_{\max-\rho}$, $\max_{\lambda} E[\rho_\lambda]$		**Max. F-measure** $\lambda_{\max-F}$ $\max_{\lambda} E[F_\lambda]$	
	SSI	BPI	SSI	BPI
(10dB,0.04,3)	(0.036,0.83)	(0.27,0.61)	(0.027,0.68)	(0.16,0.52)
(10dB,0.04,6)	(0.11,0.97)	(0.17,0.8)	(0.097,0.85)	(0.20,0.69)
(10dB,0.06,3)	(0.023,0.75)	(0.25,0.56)	(0.019,0.60)	(0.098,0.48)

method compared to the SSI. In that aspect, it may be beneficial to use structured sparse inversion techniques. We saw that different λ in (2.6) may end up in very different channels. Smart stopping criteria may also be crucial in the process for selecting the best channel estimate. In that aspect, performing wise thresholding or post-processing of the raw reflection estimate, based on probabilistic assumption, bulk of adjacent channels or some a-priori knowledge, may show improved performance

REFERENCES

[1] R.Zhang and J.Castagna, "Seismic sparse-layer reflectivity inversion using basis pursuit decomposition", Geophysics vol.76 no.6, Nov-Dec 2011

[2] SS Chen, DL Donoho et al, "Atomic decomposition by by basis pursuit: *SIAM Rev.*, 43(1), p. 129–159.

[3] M.Elad, "Sparse and Redundant Representations", Spring 2010

[4] T.Efrom, T.Hastie et al, "Least Angle Regression", Annals of Statistics 2004, Vol. 32, No. 2, 407–499

[5] R.J.Tibshirani, "The LASSO Problem and Uniqueness", Electronic Journal of statistics Volume 7 (2013), 1456-1490

[6] SpaSM- Matlab Toolbox for performing sparse regression, http://www2.imm.dtu.dk/projects/spasm/

[7] A.Heimer, I.Cohen, "Multichannel blond seismic deconvolution using dyanic programming", Journal of Signal Processing Volume Issue 7, p. 1839-1851
Volume 7 (2013), 1456-1490

[8] A.J. Berkhout, The seismic method in the search for oil andgas: current techniques and future developments, Proc.IEEE 74 (8) (August 1986) 1133–1159